Indian Journal of Ecology (2022) 49(6): 2395-2403
DOI: https://doi.org/10.55362/IJE/2022/3839

Manuscript Number: 3839
NAAS Rating: 5.79

Retrieving MODIS AOD and Evaluation of Ground-level $PM_{2.5}$ in Addition to the Identification of Potential Source Regions Over South India

Selvetikar Ashok, M. Chandra Sekhar, and D. Rama Bhupal Reddy[1]

National Institute of Technology Warangal-506 004, India
[1]GMR Institute of Technology, GMR Nagar-532 127, India
E-mail: sashok007@student.nitw.ac.in

Abstract: In this paper retrieving Aerosol Optical Depth (AOD) from Moderate Resolution Imaging Spectroradiometer (MODIS),was used to estimate the ground-level $PM_{2.5}$ in the south Indian region, the AOD and other meteorological parameters are also considered, with various grid sizes helpful to find more accurate data prediction of $PM_{2.5}$ levels. The multiple regression methods are implemented in this article, the study has shown good agreement in the prediction of $PM_{2.5}$ at the Zoopark location, all other locations are in the moderate range. $PM_{2.5}$ particle's Source identification was done based on Potential Source Contribution Function (PSCF), Concentration-Weighted Trajectory (CWT), and Cluster analysis archive the receptor dominating source regions. The Central India and East Indian regions are more dominating source regions at receptor locations in the winter season. The predominant sources are local sources at the receptor location. The cluster analysis has shown the intensity of combined trajectories towards receptor location. Winter season cluster III was dominating among the all seasons at receptor location.

Keywords: $PM_{2.5}$, MODIS, Back-Trajectory, Cluster analysis

Atmosphere Aerosols are an important role in driving the pollution at ground level, dust loading coupled with black carbon emissions from local sources in northern India (Lau et al 2006) and Aerosol loading in East Asia (Kim et al 2007). The total loading of aerosol in climate is measured based on the AOD, AE, and SSA and may be based on surrounding regions these are the sea salt aerosol (sea), volcanic eruption, natural sources, and anthropogenic activities. The aerosol loading varies with source and climate conditions. The aerosol dust is transported from far away regions in the elevated layers (<3000m) towards the receptor regions (Sun et al 2001). However, the wind speed and wind direction are the dominating transportation of aerosols, it is proved by Xia et al (2011) that the south-westerly winds are dominating the central Tibetan Plateau. The AOD represents the columnar property of the atmosphere, few studies are retrieving AOD from remote sensing instruments to understand the columnar properties, aerosol vertical profile, and estimating the $PM_{2.5}$ (Wu et al 2016, Ferrero et al 2019). The field campaign study also helpful in AOD properties, from the literature study the ISRO-GBP field campaign measured AOD with MICROTOPs instruments, fine particles dominating with the fine mode around 0.23 mm and coarse mode around 1 mm(Singh et al 2006). Badarinath et al (2007) case study showing the dust storm over the south Indian region over Hyderabad, reveals that the diffuse-to-direct-beam ratio is the most appropriate parameter for dust monitoring, the variation in AOD also observed in dust and non-dust days it influences based on local meteorology. The cloud properties effect the presence of aerosols in the atmosphere, it influences on cloud droplet number concentration based on aerosol humidification (Gryspeerdt et al 2016). The particle charge state influence atmospheric humidity, which produces liquid bridging forces and electrostatic interactions among particles that may be negative or positive in charge, the agglomeration rate of particles would increase with a rise in the atmospheric humidity (He et al 2019). Such, aerosols influence agricultural production (Greenwald et al 2006). However, biomass burning significantly affects the aerosol optical properties locally as well in the downwind regions (Shaik et al 2019). The overall aerosol properties in Indian regions change based on their production mechanisms, removal and transport processes can contribute to these variations (Ramachandran et al 2012). East Indian regions have high aerosol concentrations during winter than during summer months in an urban environment (Pani and Verma 2014). The source identification based on a Trajectory study by Shaik et al (2019) revealed the transport pathways originated from central India and adjacent oceanic regions during the post-monsoon season. Ramachandran (2005) showed that the long-range transport of pollutants from the surrounding continental locations was found unhealthy indicating the influence of anthropogenic pollution. Banerjee et al (2015) concluded that based on a review of receptor models used in India, vehicular pollutions are dominating in Hyderabad region. The trajectory based approach identifies the source regions. In this article, assessment of the suitable MODIS instrument Terra/Aqua AOD and Meteorological parameters, to identify the ground-level $PM_{2.5}$ based on the multiple regression analysis over Hyderabad. The missing gaps filled with predicted $PM_{2.5}$and identified the potential sources of receptor location, based on backward trajectories, were CWT, PSCF, and cluster analysis are used in this study.

MATERIAL AND METHODS

Study area and source regions: In this study south Indian region, Hyderabad was chosen, Hyderabad city was developed and the urban city was full of traffic and industrial areas surrounded. The pollution may be due to local source regions dominating as well as transport of pollutants may influence the pollution in the city region. The average annual rainfall is 136.1 mm, average altitude of 542 meters, the highest being Banjara Hills at 672 meters. Hyderabad has the surrounding with different regions such as Industrial and rural areas, whereas the CPCB monitoring location (Fig. 1) operates under Telangana state pollution control Board (TSPCB). The region is full of developed area so the pollution is under control such that continuous monitoring stations are very useful for the assessment of urban impact. The study region is located in south Indian region which was Deccan tebetaian. The study region domination pollutants are the vehicular activities and nearby industrial sources, building contraction and metro construction emissions such anthropogenic sources are main contributions of Hyderabad pollution levels as well as the outside the city agriculture burning and wast burning around the city are the secondary level sources but the effect of all these sources transport by the wind from far away regions. The boundary states are Maharashtra in north, Karnataka in west, Andhra Pradesh in the south, Chahattisgarh states are east side located for Telangana state. Patancher industrial area located North West direction, small and medium industries are sourended by 40 km from the center of city Hyderabad, all other sides are agriculture land bounded. The biomass burning of Agriculture waste burning maybe influence.

MODIS AOD data collection: The satellite AOD product is provided by the Moderate Resolution Imaging Spectroradiometer (MODIS) on the Terra/Aqua instrument (Levy and Hsu et al 2017). The MODIS instrument is a multi-spectral radiometer, designed to retrieve aerosol microphysical and optical properties over land and ocean. The MODIS instrument produces global coverage in 1 or 2 days and captures most of the aerosol variability due to this high sampling frequency. In this study, the MODIS level 2 daily AOD data from Terra (MOD04_3K, MOD04_L2 Collection 6.1) and Aqua (MYD04_3K, MYD04_L2) are used, which is reported at 3K for 3Km and L2 for 10km. Were used the instated of missing AOD, 3x3 or 5x5 grid product. The MODIS AOD data product was downloaded from NASA LAADS (https://ladsweb.modaps.eosdis.nasa.gov/).

Meteorological data collection: The meteorological data was adapted from CPCB (https://app.cpcbccr.com/ccr /#/caaqm-dashboard-all/caaqm-landing) at Hyderabad. The meteorological parameters are temperature, humidity, pressure, wind speed, and wind direction and $PM_{2.5}$ are secondary data collectedfrom May 2018 to May 2019.

Backward trajectory: Global Data Assimilation System (GDAS) was used as meteorological data input to the model Hysplite trajectory (Stein et al 2015). The 7-day back trajectories at a height of the surface layer (100,500 and 1000 m) archive for source analysis. Stein et al (2015) highlight the recent applications of the HYSPLIT modeling system, including the simulation of atmospheric tracer release experiments, radionuclides, smoke originating from wildfires,

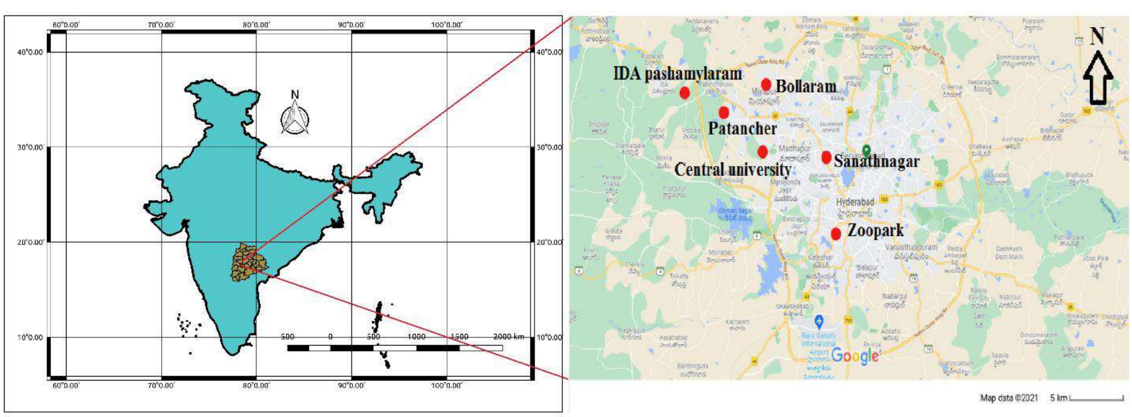

Fig. 1. Study location Hyderabad (six locations)

volcanic ash, mercury, and wind-blown dust. The back trajectories to very sophisticated computations of transport, mixing, chemical transformation, and deposition of pollutants and hazardous materials. Based on the above-generated 7-day-backward trajectories, the PSCF, CWT, and Cluster analysis were analyzed using the TrajStat tool (Wang et al 2009). The spatial resolution was 0.5×0.5° established to find the source paths. The PSCF grid values in the study domain are calculated by counting the segment endpoints. the outliers are removed based on IQR and Z-score methods. The filtered data was divided into 80% for model fitting and 20% for validation. The AOD and meteorology influence PM 2.5 concentration near ground level, were as the multiple regression analysis was used to predict the $PM_{2.5}$ at six locations in Hyderabad, the MODIS data extracted based on Python scripts, were as 5x5 and 3x3 grid data considered for fill the gaps in average grid AOD. The model validation based on statistical parameters (RMSE, NMB, d, and R) concluded the best fit model for MODIS collection.

The CWT, PSCF, and Cluster analysis based on predicted $PM_{2.5}$ concentrations identified the sources of $PM_{2.5}$ near the study region. The 7-day back-trajectories data from Hysplite model was archived. The whole study was divided based on the Indian meteorology department (IMD) four seasons (winter, pre-monsoon, Monsoon, and Post-monsoon). The layers are identified as long-range transport of dust at the receptor location. The threshold criterion for $PM_{2.5}$ was 60 ug/m^3 in PSCF. Han et al(2007)gave the calculation of endpoints in a particular grid cell, which allowed for calculating the PSCF. In the CWT method, each grid cell is assigned a weighted concentration by averaging the sample concentration. The trajectory endpoint time in the grid cells has been weighted by the $PM_{2.5}$ corresponding trajectory. Cluster analysis based on the Ecudian methodology was used in this study to cluster the seasonal dominant paths and contribution areas. The clustering technique shows the average trajectory paths.

RESULTS AND DISCUSSION

Variation of AOD and meteorological parameters: The AOD was maximum at Bollarm (0.54) and minimum in Zoopark (0.47) observed in this study. The meteorology of the six locations (Fig. 2) with standard deviations shows that the $PM_{2.5}$, AOD, BP, and SR parameters are more deviations at all locations but theless deviation within Ambient Temperature (AT), Relative humidity (RH). It may be due to the topography of land and climate conditions and as well as the long-range transport of the pollutants.

MODIS AOD for prediction of the $PM_{2.5}$: AOD-$PM_{2.5}$relation was a great correlation observed in some locations. The

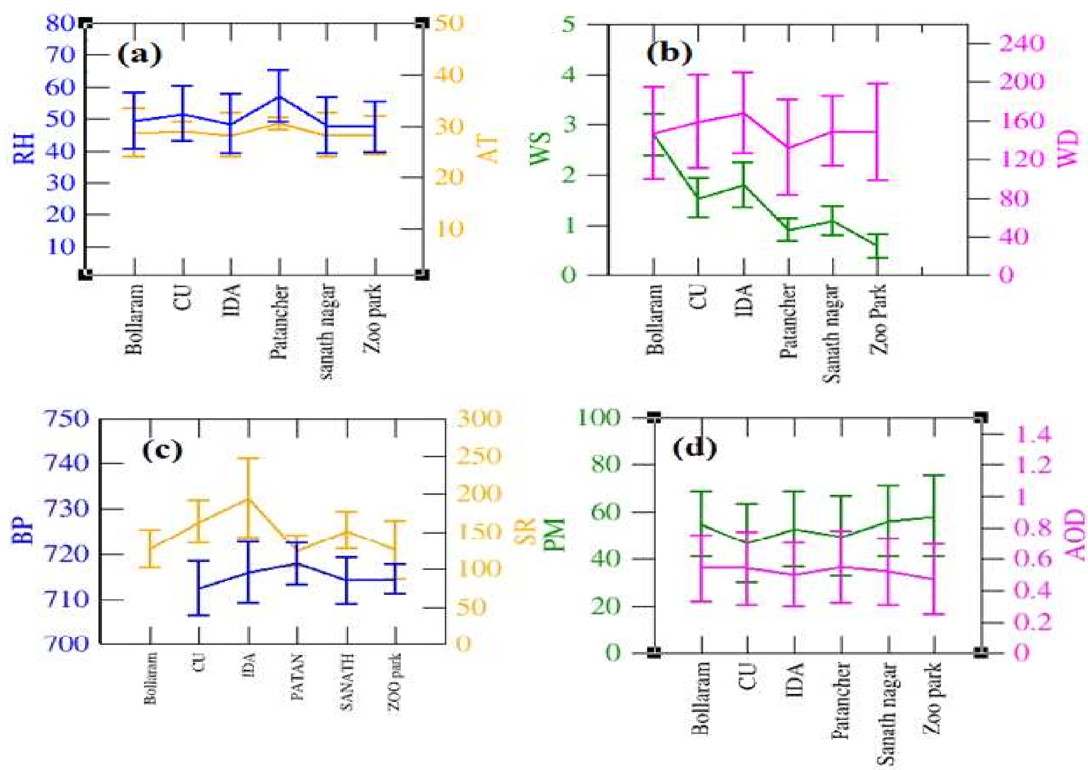

Fig. 2. Meteorological variation of all locations

MODIS all products (MOD_3K, MOD_L2, MYOD_3K, and MYOD_L2) had good correlations at Zoo park observed in this study. The Patancher and IDA locations are moderate correlation seen, other locations are below moderately correlation observed, it may be due to different meteorology around the regions and as well as the land properties are more uncertain in MODIS AOD retrievals (Sathe et al 2019).

The correlation coefficient R, RMSE, d, and NMB model validation parameters are shown (Table 1) the best-fit combination. The statistical parameters are used(Sathe et al

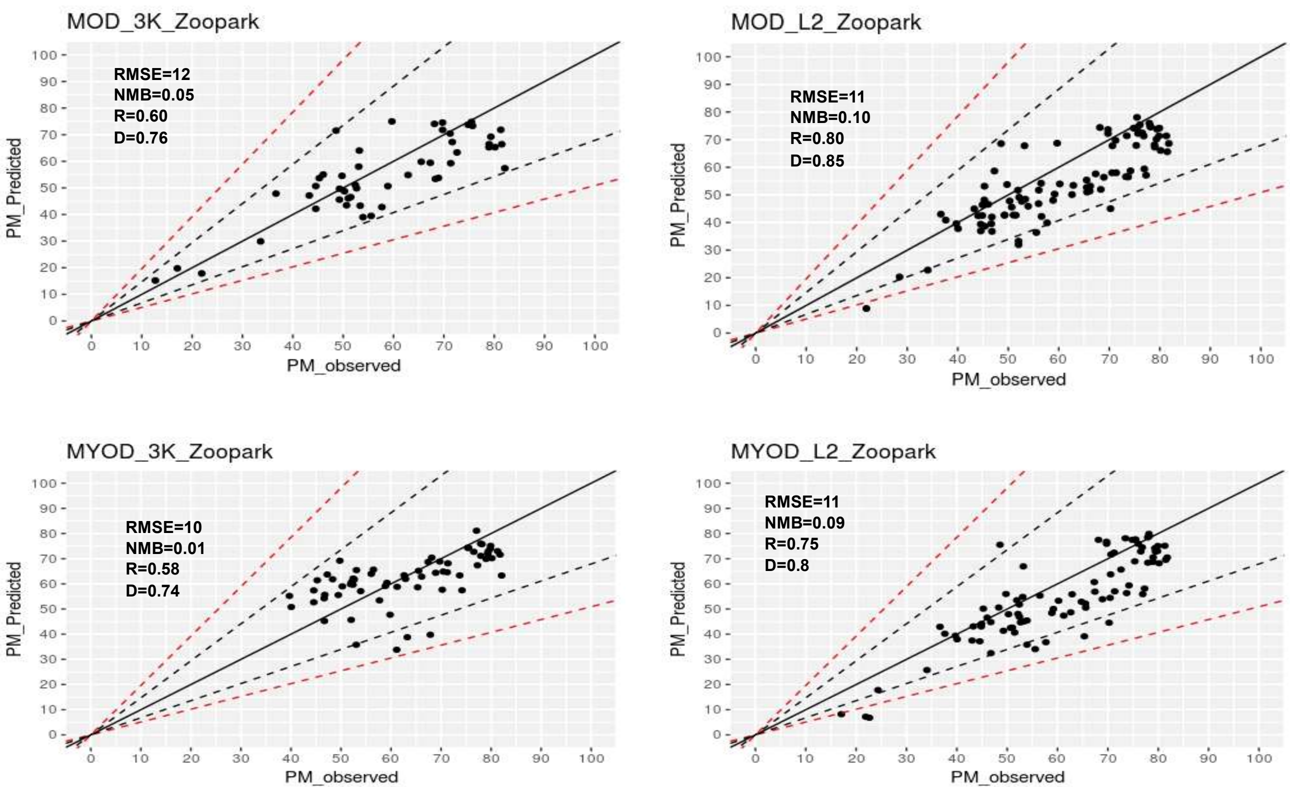

Fig. 3. Scatter plot for $PM_{2.5}$Predicted and Observed at Zoopark location for four MODIS AOD

Table 1. Model performance statistical parameters

	Parameter	Bollaram	Central univercity	IDA	Patancher	Sanath nagar	Zoo park
MOD_3K	RMSE	15	15	11	54	10	12
	D	0.53	0.59	0.81	0.21	0.78	0.76
	NMB	-0.15	-0.02	-0.02	-0.84	-0.04	0.05
	R	0.37	0.36	0.37	-0.43	0.69	0.60
MOD_L2	RMSE	12	14	12	55	11	11
	D	0.52	0.66	0.71	0.22	0.73	0.85
	NMB	-0.009	0.11	-0.03	-0.87	-0.03	0.10
	R	0.59	0.55	0.68	-0.39	0.62	0.80
MYOD_3K	RMSE	15	15	13	47	10	10
	D	0.52	0.73	0.62	0.25	0.81	0.74
	NMB	-0.12	0.14	-0.08	-0.67	-0.02	0.01
	R	0.53	0.46	0.42	-0.34	0.45	0.58
MYOD_L2	RMSE	14	16	11	44	11	11
	D	0.52	0.60	0.82	0.22	0.74	0.80
	NMB	-0.12	0.11	-0.04	-0.67	-0.01	0.09
	R	0.46	0.40	0.70	-0.50	0.65	0.75

2019) to identify the model performance. MOD_3K has all locations are negative NMB indicating except Zoopark the negative shows that models are in general estimating lower $PM_{2.5}$ concentration than observed the model was under predicting $PM_{2.5}$. For positive indicate that over predicting the $PM_{2.5}$ concentration than observed values. The correlation coefficient higher values shown at Zoopark were as low as the correlation shown in other regions. The RMSE has seen higher (54 ug/m^3) at Patancheru and other locations low in range (11-15 µg/m^3), Here we observed that the Patancheru RMSE value has peaked in all MODIS collections compared to other locations. The correlation was great at the Zoopark and lower relation at Patancheru. The RMSE variation range (11-14µg/m^3) except the Patancheru region. The MYOD_3K and MYOD_L2 have nearly similar values in RMSE, d, and NMB, where the good agreement in correlation coefficient in the MOD_L2 product was seen. the scatter plot for the Zoopark location (Fig. 3) the best fit model data from multiple regression analysis, it is seen from the model validation analysis. The scatter plot shows the 3% and 5% percentage error line from the standard line (0 % error), were as the most of the points within 3% error line, few points are above the 5% in MYOD_L2 product, the grater resolution data have more deviation from the standard line seen in this study.

Back Trajectory Analysis for Source Identification

Concentration-Weighted Trajectory (CWT): The CWT analysis (Fig. 4a, b, c, d) form all seasons identified in the winter season was dominating among the all seasons. The weighted trajectory paths are seen from East India regions and coastal regions are major sources. Were as other seasons being weightage of trajectory seen to be less. The pre-monsoon identifies the two paths which are from land and sea regions, which effect may be due to land and sea breeze effect nearby coastal regions, the one path from central India and the other is from the Bay of Bengal. The monsoon season will be a dominating trajectory from West India and the Arabian Sea. The post-monsoon will be affected by East Indian regions. The two seasons (winter and pre-monsoon) have two identification paths and the other two (monsoon and post-monsoon) have one transport path.

Potential Source Contribution Function (PSCF): The potential source contribution function shows the receptor source regions, shows the all seasons PSCF (Fig. 5 I, II, III, and IV) for Winter, pre-monsoon, monsoon, and post-monsoon seasons. The winter season sources are from coastal and East regions, were as the pre-monsoon contribution source areas seen to be high from sea regions other from the West region. There are very low source regions in monsoon and post-monsoon seasons.

Cluster analysis: Trajectory cluster analysis was applied to identify the clustering of the seasonal base analysis of the study period at the receptor location. The Winter, pre-monsoon, monsoon and post-monsoon seasons (Fig. 6 a, b, c and d) were presented. The legend shows the height of the trajectory with respective each cluster. The each cluster's contribution (Table 2) towards the receptor site in

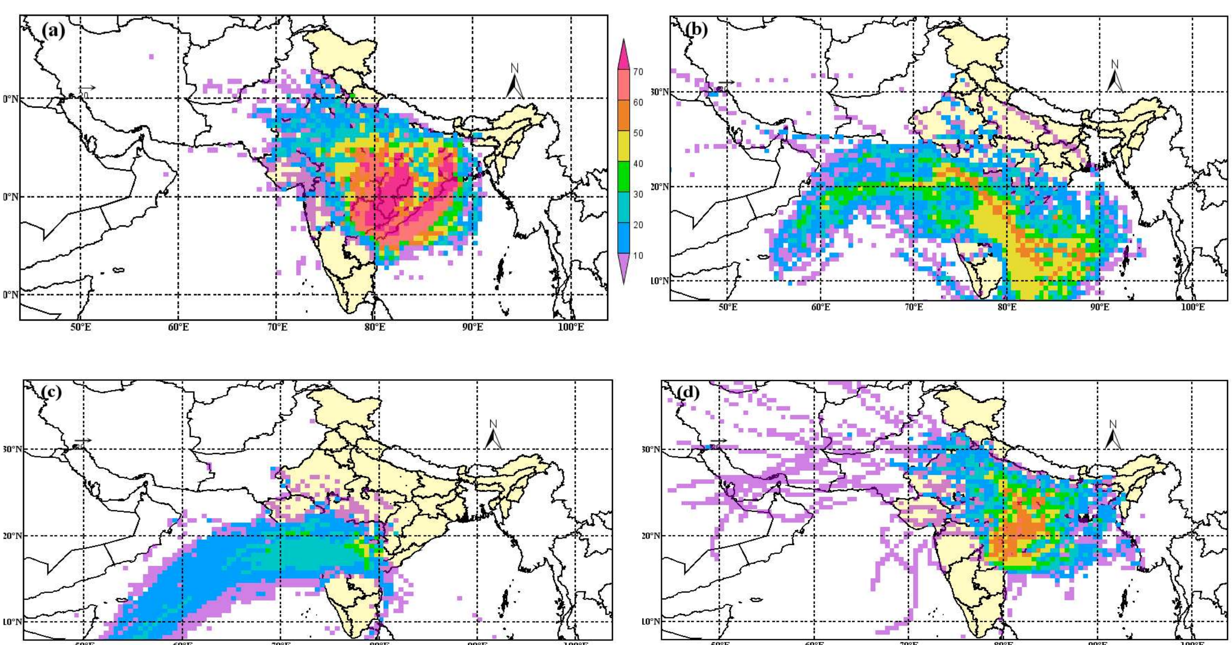

Fig. 4. CWT analysis with different seasons (same scale for all figures follows the Figure (a) legend).

percentage, with six clusters divided based on the direction. The clusters are dominating central India and North West Indian regions in the winter season. The pre-monsoon season has different direction clusters but the Bay of Bengal has the low-level trajectories seen in this season. The monsoon season has all clusters from the Arabian Sea region and West India. Most of the trajectories are from local regions, the Winter polluted cluster was Cluster I, the mean concentration as 72.05 μg/m^3 but the number of polluted trajectories is 179 which is the highest number of the trajectory seen in Winter season. The least polluted trajectory means 34.64μg/m^3 associated with cluster III in monsoon. The polluted clusters has the less number of trajectories but the intensity of pollutant transport is more, compared to other clusters.

Reduction in $PM_{2.5}$ under high RH due to the deposition of

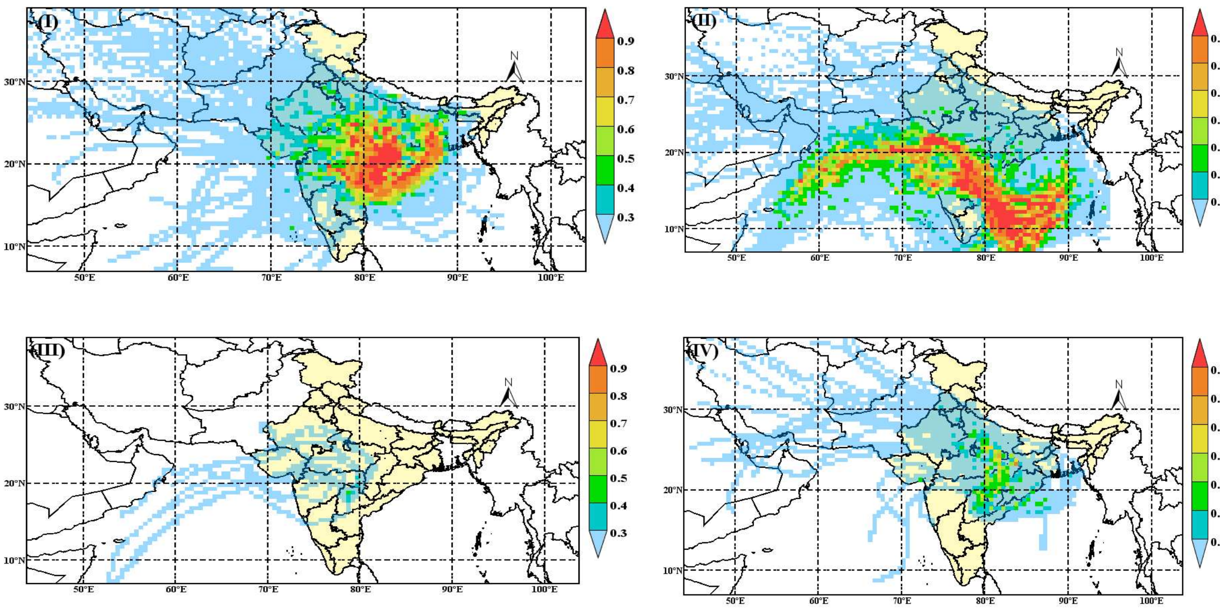

Fig. 5. PSCF analysis with different seasons at surface layer and elevated layer

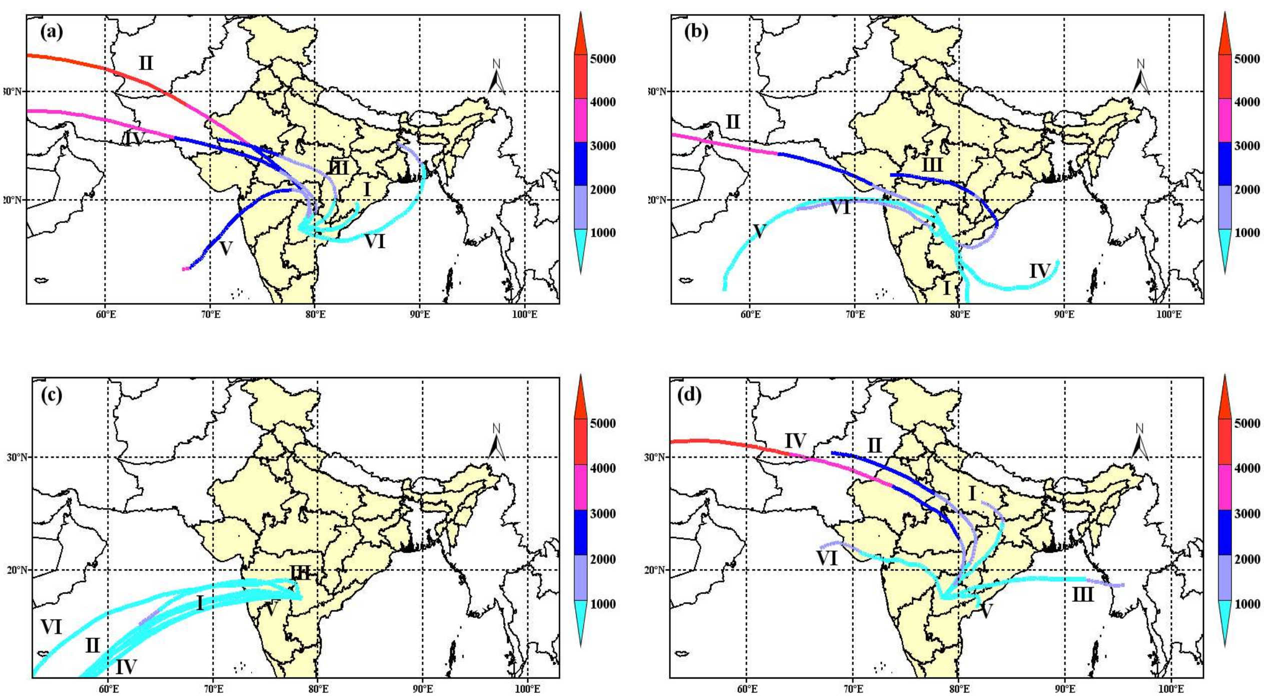

Fig. 6. Cluster analysis with different seasons at surface layer and elevated layer

Table 2. Polluted clusters and associated trajectory's numbers

Winter	Number_traj	Mean_value	Standard devation	Polluted_num	Polluted_mean_value	Polluted_stdev	Ratio (%)
1	202	72	8.4	179	74.2	4.3	21.6
2	45	65	11.6	29	72.1	5.5	8.33
3	79	68	10.3	61	72.5	5.8	38.1
4	163	64	12.4	98	73.3	5.5	13.52
5	42	63	14.3	26	73.4	5.9	7.22
Pre_monsoon							
1	118	43	7.6	0	0	0	18.29
2	49	48	10.8	6	69.4	7.8	7.91
3	51	50	10.4	9	66.4	4	7.91
4	199	48	11.3	38	66.9	4.4	31.3
5	115	42	11.5	11	67.8	7.7	19.22
6	98	47	9.7	11	66.7	5.9	15.3
Monsoon							
1	154	21	5.6	0	0	0	22.59
2	89	25	7.4	0	0	0	12.4
3	111	34	12.7	10	62.4	2.7	17.15
4	124	18	3.2	0	0	0	18.9
5	133	21	4.2	0	0	0	20.9
6	55	32	9.2	2	63.1	4.8	7.95
Post monsoon							
1	97	55	19.2	42	71.1	6.4	29.23
2	60	50	23.9	24	70.1	5.4	17.76
3	55	40	13.2	4	67.8	5.1	15.03
4	26	54	25.7	15	72.6	5.1	8.20
5	67	42	22.3	16	69.1	6.1	22.40
6	16	33.33	27.28	4	72.18	7.53	7.38

dust particles, the high average temperature in the patancheru area (30.51^{oC}) observed may be due to the industrial zone. The temperature inversion leads to higher values of pollutants in the winter season (Yadav et al 2019), PSCF has shown high source regions in the winter season compared to other seasons. The variation of meteorology gives the climate change in the northeast region (Deb and Sil 2019). Numerous studies also shown that meteorology is a great influence on the ground level particulate concentration and transboundary aerosols (Tiwari et al 2015, Yadav et al 2016). As well as several studies show that the correlation between AOD and ground-level $PM_{2.5}$ concentration and estimation of Particulate matters from AOD (Lv et al 2017, Shao et al 2017, Lu et al 2021, Tuna et al 2021).

Previous studies are shown based on back trajectory analysis of effective origin source regions and long-range transport of pollutants (Conte et al 2020, Hong et al 2019, Owega et al 2006). The satellite retrieval studies shown the better agreemt for hydrometeorological studies (Suchithra and Agarwal 2021). Road dust particles are effecting on Plant Species (Bemmansour et al 2021). Soni et al (2018) reported that the $PM_{2.5}$ and AOD nonlinear multi-regression model performance was better for the Jaipur region. The AOD influences the cloud properties (Balakrishnaiah et al 2012, Kumar 2013, Gopal et al 2016,).The observational study has shown the AOD-$PM_{2.5}$over china region (Xin et al 2016) concluded that there was a high consistency of AOD versus $PM_{2.5}$ and the correlation coefficient ranges from 0.64 to 0.70 across China. The European hot-spot areas are identified by Squizzato and Masiol (2015)based on the statistical approaches to understand the influence of external and local contribution of $PM_{2.5}$sources such as back-trajectories cluster analysis, PSCF, and CWT analysis, here we are also concluded that the most dominating sources based on trajectory calculation, and in our study. The back-trajectory-based source apportionment of airborne sulfur and nitrogen concentrations identified the source contribution at the receptor (Gebhart et al 2011). The dust outbreaks are identified in Spain (Cabello et al 2016). The tracking of Hazardous air pollutants from refinery fire based on trajectory by Shie and Chan (2013). The comparative study within two cities was analyzed for source identification (Kong et al 2013).

In this study found that the high contribution regions from East Indian regions and coastal regions in Winter season, the pre-monsoon origins from Bay of Bengal and central Indian regions, the most of air mass transport from these regions.

CONCLUSIONS

In this study, the assessment of ground-level $PM_{2.5}$ is based on meteorology and MODIS AOD. The multiple regression analysis was adopted in this study. The good perdition of $PM_{2.5}$at the Zoo park location was found, were as other locations are in the moderate range. On the other hand, source identification based on trajectory-based analysis as CWT, PSCF, and cluster analysis has shown in this study, the long-range transport of the $PM_{2.5}$and potential source regions from the East India and Coastal regions are the potential source regions at receptor locations, among all seasons winter season local pollutant are dominating. It is maybe due to anthropogenic and vehicular activities. The cluster analysis provided the main mechanism of similar types of trajectories transporting paths towards the receptor. Cluster III in the winter season was dominating at receptor location. The study was useful for the health policymakers to establish new guidelines. As well as the pollution assessment of the remote location.

ACKNOWLEDGMENTS

The authors gratefully acknowledge the NOAA Air Resources Laboratory (ARL) for the provision of the HYSPLIT transport and dispersion model and/or READY website (*https://www.ready.noaa.gov*) and Central pollution control Board (CPCB) Provided the meteorology data used in this publication.

REFERENCES

Badarinath KVS, Kharol SK, Kaskaoutis DG, and Kambezidis HD 2007. Case study of a dust storm over Hyderabad area, India: Its impact on solar radiation using satellite data and ground measurements. *Science of the Total Environment* **384**(1-3): 316-332.

Balakrishnaiah G, Raghavendra kumar K, Suresh Kumar Reddy B, Rama Gopal K, Reddy RR, Reddy LSS, Swamulu C, Nazeer Ahammed Y, Narasimhulu K, KrishnaMoorthy K and Suresh Babu S 2012. Spatio-temporal variations in aerosol optical and cloud parameters over Southern India Retrieved from MODIS Satellite Data. *Atmospheric Environment* **47**: 435-445.

Banerjee T, Murari V, Kumar M, and Raju MP 2015. Source apportionment of airborne particulates through receptor modeling: Indian scenario. *Atmospheric Research* **164-165**: 167-187.

Bemmansour EH, Bouyakoub ZA, Harrache D, and Bemmansour N 2021. Detection of air pollution of road origin by a bio-accumulating plant species (*Pinus Halepensis*) and evaluation of the concentrations of heavy metals in Western Algeria. *Indian Journal of Ecology* **48**(2): 472–477.

Cabello M, Orza JAG, Dueñas C, Liger E, Gordo E, and Cañete S 2016. Back-trajectory analysis of African dust outbreaks at a coastal city in Southern Spain: Selection of starting heights and assessment of african and concurrent mediterranean contributions. *Atmospheric Environment* **140**: 10-21.

Conte M, Merico E, Cesari D, Dinoi A, Grasso FM, Donateo A, Guascito MR, and Contini D 2020. Long-term characterisation of African dust advection in South-Eastern Italy: Influence on fine and coarse particle concentrations, size distributions, and carbon content. *Atmospheric Research* **233**: 104690.

Deb S and Sil BS 2019. Climate change study for the meteorological variables in the Barak River Basin in North-East India. *Urban Climate* **30**: 100530.

Ferrero L, Riccio A, Ferrini BS, D'Angelo L, Rovelli G, Casati M, Angelini F, Barnaba F, Gobbi GP, Cataldi M, and Bolzacchini E 2019. Satellite AOD conversion into ground PM10, PM25 and PM1 over the Po Valley (Milan, Italy) exploiting information on aerosol vertical profiles, chemistry, hygroscopicity and meteorology. *Atmospheric Pollution Research* **10**(6): 1895-1912.

Gebhart KA, Schichtel BA, Malm WC, Barna MG, Rodriguez MA, and Collett JL 2011. Back-trajectory-based source apportionment of airborne sulfur and nitrogen concentrations at Rocky Mountain National Park, Colorado, USA. *Atmospheric Environment* **45**(3): 621-633.

Gopal KR, Obul Reddy KR, Balakrishnaiah G, Arafath SMd, Kumar Reddy NS, Rao TC, Reddy TL and Reddy RR 2016. Regional trends of aerosol optical depth and their impact on cloud properties over Southern India using MODIS data. *Journal of Atmospheric and Solar-Terrestrial Physics* **146**: 38-48.

Greenwald R, Bergin MH, Xu J, Cohan D, Hoogenboom G, and Chameides WL 2006. The influence of aerosols on crop production: A study using the CERES crop model. *Agricultural Systems* **89**(2-3): 390-413.

Gryspeerdt E, Quaas J and Bellouin N 2016. Constraining the aerosol influence on cloud fraction: AEROSOLS and cloud fraction. *Journal of Geophysical Research: Atmospheres* **121**(7): 3566-3583.

Han Y-J, Holsen TM, and Hopke PK 2007. Estimation of source locations of total gaseous mercury measured in New York State using trajectory-based models. *Atmospheric Environment* **41**(28): 6033-6047.

He Y, Gu Z, Lu W, Zhang L, Okuda T, Fujioka K, Luo H, and Yu CW 2019. Atmospheric humidity and particle charging state on agglomeration of aerosol particles. *Atmospheric Environment* **197**: 141-149.

Hong Q, Liu C, Hu Q, Xing C, Tan W, Liu H, Huang Y, Zhu Y, Zhang J, Geng T and Liu J 2019. Evolution of the vertical structure of air pollutants during winter heavy pollution episodes: The role of regional transport and potential sources. *Atmospheric Research* **228**: 206-222.

Kim SW, Yoon SC, Kim J and Kim SY 2007. Seasonal and monthly variations of columnar aerosol optical properties over East Asia determined from multi-year MODIS, LIDAR, and AERONET Sun/Sky radiometer measurements. *Atmospheric Environment* **41**(8): 1634-1651.

Kong X, He W, Qin N, He Q, Yang B, Ouyang H, Wang Q and Xu F 2013. Comparison of transport pathways and potential sources of PM10 in two cities around a large Chinese Lake using the modified trajectory analysis. *Atmospheric Research* **122**: 284-297.

Kumar A 2013. Variability of aerosol optical depth and cloud parameters over North Eastern regions of India retrieved from MODIS satellite data. *Journal of Atmospheric and Solar-Terrestrial Physics* **100-101**: 34-49.

Lau KM, Kim MK and Kim KM 2006. Asian summer monsoon anomalies induced by aerosol direct forcing: The role of the Tibetan plateau. *Climate Dynamics* **26**(7–8): 855-864.

Levy R and Hsu C et al 2017. MYD04_L2 MODIS/Aqua Aerosol 5-Min L2 Swath 10km

Lu X, Wang J, Yan Y, Zhou L and Ma W 2021. Estimating hourly PM25 concentrations using Himawari-8 AOD and a DBSCAN-modified deep learning model over the YRDUA, China. *Atmospheric Pollution Research* **12**(2): 183-192.

Lv B, Hu Y, Chang HH, Russell AG, Cai J, Xu B and Bai Y 2017. Daily estimation of ground-level PM25 concentrations at 4 Km resolution over Beijing-Tianjin-Hebei by Fusing MODIS AOD and ground observations. *Science of the Total Environment* **580**: 235-244.

Owega S, Khan B-U-Z, Evans GJ, Jervis RE and Fila M 2006. Identification of long-range aerosol transport patterns to toronto via classification of back trajectories by cluster analysis and neural network techniques. *Chemometrics and Intelligent Laboratory Systems* **83**(1): 26-33.

Pani SK and Verma S 2014. Variability of winter and summertime aerosols over Eastern India urban environment. *Atmospheric Research* **137**: 112-124.

Ramachandran S 2005. PM mass concentrations in comparison with aerosol optical depths over the Arabian sea and Indian ocean during winter monsoon. *Atmospheric Environment* **39**(10): 1879-1890.

Ramachandran S, Kedia S and Srivastava R 2012. Aerosol optical depth trends over different regions of India. *Atmospheric Environment* **49**: 338-347.

Sathe Y, Kulkarni S, Gupta P, Kaginalkar A, Islam S and Gargava P 2019. Application of Moderate Resolution Imaging Spectroradiometer (MODIS) Aerosol Optical Depth (AOD) and Weather Research Forecasting (WRF) Model Meteorological Data for Assessment of Fine Particulate Matter (PM25) over India. *Atmospheric Pollution Research* **10**(2): 418-434.

Shaik DS, Kant Y, Mitra D, Singh A, Chandola HC, Sateesh M, Babu SS and Chauhan P 2019. Impact of biomass burning on regional aerosol optical properties: A case study over Northern India. *Journal of Environmental Management* **244**: 328-343.

Shao P, Xin J, An J, Kong L, Wang B, Wang J, Wang Y, and Wu D 2017. The empirical relationship between PM25 and AOD in Nanjing of the Yangtze River Delta. *Atmospheric Pollution Research* **8**(2): 233-243.

Shie R-H and Chan C-C 2013. Tracking hazardous air pollutants from a refinery fire by applying on-line and off-line air monitoring and back trajectory modeling. *Journal of Hazardous Materials* **261**: 72-82.

Singh S, Singh B, Gera BS, Srivastava MK, Dutta HN, Garg SC, and Singh R 2006. A study of aerosol optical depth in the Central Indian region (173-86°N) during ISRO-GBP field campaign. *Atmospheric Environment* **40**(34): 6494-6503.

Soni M, Payra S and Verma S 2018. Particulate matter estimation over a semi arid region Jaipur, India using satellite AOD and meteorological parameters. *Atmospheric Pollution Research* **9**(5): 949-958.

Squizzato S and Masiol M 2015. Application of meteorology-based methods to determine local and external contributions to particulate matter pollution: A case study in Venice (Italy). *Atmospheric Environment* **119**: 69-81.

Stein AF, Draxler RR, Rolph GD, Stunder BJB, Cohen MD and Ngan F 2015. NOAA's HYSPLIT atmospheric transport and dispersion modeling system. *Bulletin of the American Meteorological Society* **96**(12): 2059-2077.

Suchithra AS and Agarwal S 2021. Intercomparison of trend analysis using multi satellite precipitation products and gauge measurements. *Indian Journal of Ecology* **48**(4): 955-963.

Sun J, Zhang M and Liu T 2001. Spatial and temporal characteristics of dust storms in china and its surrounding regions, 1960-1999: Relations to source area and climate. *Journal of Geophysical Research: Atmospheres* **106**(D10): 10325-10333

Tiwari S, Pandithurai G, Attri SD, Srivastava AK, Soni VK, Bisht DS, Anil Kumar V and Srivastava MK 2015. Aerosol optical properties and their relationship with meteorological parameters during wintertime in Delhi, India. *Atmospheric Research* **153**: 465-479.

Tuna Tuygun G, Gündoğdu S and Elbir T 2021. Estimation of ground-level particulate matter concentrations based on synergistic use of MODIS, MERRA-2 and AERONET AODs over a coastal site in the Eastern Mediterranean. *Atmospheric Environment* **261**: 118562.

Wang YQ, Zhang XY and Draxler RR 2009. TrajStat: GIS-based software that uses various trajectory statistical analysis methods to identify potential sources from long-term air pollution measurement data. *Environmental Modelling & Software* **24**(8): 938-939.

Wu J, Yao F, Li W and Si M 2016. VIIRS-based remote sensing estimation of ground-level PM25 concentrations in Beijing–Tianjin–Hebei: A spatiotemporal statistical model. *Remote Sensing of Environment* **184**: 316-328.

Xia X, Zong X, Cong Z, Chen H, Kang S, and Wang P 2011. Baseline continental Aerosol over the Central Tibetan Plateau and a case study of aerosol transport from South Asia. *Atmospheric Environment* **45**(39): 7370-7378.

Xin J, Gong C, Liu Z, Cong Z, Gao W, Song T, Pan Y, Sun Y, Ji D, Wang L, Tang G and Wang Y 2016. The observation-based relationships between PM_{25} and AOD over China: The functions of PM_{25} AND AOD over China. *Journal of Geophysical Research: Atmospheres* **121**(18): 10,701-10,716.

Yadav R, Sahu LK, Beig G and Jaaffrey SNA 2016. Role of long-range transport and local meteorology in seasonal variation of surface ozone and its precursors at an urban site in India. *Atmospheric Research* **176-177**: 96-107.

Yadav R, Sahu LK, Beig G, Tripathi N, Maji S and Jaaffrey SNA 2019. The role of local meteorology on ambient particulate and gaseous species at an urban site of Western India. *Urban Climate* **28**: 100449.

Received 30 July, 2022; Accepted 27 October, 2022